Newport Beach, CA, USA
ACTIVE 95
1995 July 06–08

ACTIVE CONTROL OF STRUCTURAL INTENSITY IN CONNECTED STRUCTURES

Moongyung Nam *, Sabih I. Hayek *, and Scott D. Sommerfeldt #

***Department of Engineering Science and Mechanics, # Graduate Program in Acoustics, Penn State University, University Park, PA, 16802**

INTRODUCTION

Flexural vibration energy from machinery can be transmitted through a structure, such as a panel, to a connected beam-like structure. The connected structure can dissipate this energy through coupling to an acoustic medium or to other structures. The objective of this work is to prevent the energy from flowing to the connection point. An elastic plate is connected to another structure with a resistive connection point impedance. The elastic plate is excited to vibration by a point load at a single frequency. The point force is located at a certain position and acts as the primary mechanical source of vibration for an internally damped, simply supported plate. A point damper, representing a resistively connected structure, located at another position, acts as an energy sink which models the power flow transmission to a connected beam-like structure. The damping coefficient of the point damper represents the degree of energy transmission at the connection point. A control force is applied to the plate in order to reduce the structural intensity (SI) at the point damper location.

The analysis and measurement of SI has been studied by few authors. The measurement of SI has been reported in Ref[1-6]. Analytical studies of active control of power flow in beams and plates, and shells were reported in Ref.[7-16], and experimental studies in Ref.[17-20].

STRUCTURAL INTENSITY IN A CONNECTED PLATE

The structural intensity vector is the mechanical power flow per vector unit area, which has direction and magnitude as a function of position in the structure. Thus, a structural intensity map, being composed of structural intensity vectors, shows the power flow from an energy source to all points in the plate. The real part of the structural intensity is the active intensity and propagates along the structure representing the net power flow. The x- and y- components of the instantaneous structural intensity vector of an elastic plate obeying the Bernoulli-Euler theory can be expressed as

$$I_x(x,y,t) = -\left(V_x \frac{\partial W}{\partial t} + M_x \frac{\partial \Theta_x}{\partial t} + M_{yx} \frac{\partial \Theta_y}{\partial t} \right)$$
$$I_y(x,y,t) = -\left(V_y \frac{\partial W}{\partial t} + M_y \frac{\partial \Theta_y}{\partial t} + M_{yx} \frac{\partial \Theta_x}{\partial t} \right) \qquad (1)$$

The first term of eq. (1) is the product of the shear force and the transverse velocity. The second term is the product of the bending moment and the associated angular velocity. The third term is the product of the twisting moment and the associated angular velocity. The bending moments (M_x, M_y), the twisting moment M_{xy}, the transverse shear forces (V_x, V_y) and the rotational displacements (Θ_x, Θ_y) can be expressed in terms of the spatial derivatives of the transverse displacement $W(x,y,t)$. With conventional sign notation, these are given by :

$$M_x = -D\left(\frac{\partial^2 W}{\partial x^2} + \nu\frac{\partial^2 W}{\partial y^2}\right) \quad M_y = -D\left(\frac{\partial^2 W}{\partial y^2} + \nu\frac{\partial^2 W}{\partial x^2}\right)$$

$$V_x = -D\frac{\partial}{\partial x}\left(\frac{\partial^2 W}{\partial x^2} + \frac{\partial^2 W}{\partial y^2}\right) \quad V_y = -D\frac{\partial}{\partial y}\left(\frac{\partial^2 W}{\partial x^2} + \frac{\partial^2 W}{\partial y^2}\right)$$

$$M_{xy} = M_{yx} = -D(1-\nu)\left(\frac{\partial^2 W}{\partial x \partial y}\right) \qquad (2)$$

$$\Theta_x = -\frac{\partial W}{\partial x} \quad \Theta_y = -\frac{\partial W}{\partial y}$$

Here D is the bending rigidity, given by $D = Eh^3/12(1-\nu^2)$, where ν is Poisson's ratio, E is the Young's modulus of the material, and h is the plate thickness. Inserting eq. (2) into eq. (1), one can express the structural intensity components for a thin plate in terms of the transverse displacement $W(x,y,t)$. If complex quantities are used to represent a field with simple harmonic time dependence, the time-averaged complex structural intensity ,$\vec{\tilde{I}}$, can be defined as:

$$\begin{aligned}\vec{\tilde{I}}(x,y) &= \tilde{I}_x(x,y)\,\vec{e}_x + \tilde{I}_y(x,y)\,\vec{e}_y \\ &= (\bar{I}_x(x,y) + j\overline{Q}_x(x,y))\,\vec{e}_x + (\bar{I}_y(x,y) + j\overline{Q}_y(x,y))\,\vec{e}_y\end{aligned} \qquad (3)$$

where the x- and y-components are expressed by

$$\begin{aligned}\tilde{I}_x(x,y) &= \frac{1}{2}j\omega\left\{\tilde{V}_x(x,y)\tilde{W}^*(x,y) + \tilde{M}_x(x,y)\tilde{\Theta}_x^*(x,y) + \tilde{M}_{xy}(x,y)\tilde{\Theta}_y^*(x,y)\right\} \\ \tilde{I}_y(x,y) &= \frac{1}{2}j\omega\left\{\tilde{V}_y(x,y)\tilde{W}^*(x,y) + \tilde{M}_y(x,y)\tilde{\Theta}_y^*(x,y) + \tilde{M}_{xy}(x,y)\tilde{\Theta}_x^*(x,y)\right\}\end{aligned} \qquad (4)$$

Here, the bar (-) denotes the time averaged values, the tilde (~) denotes complex quantities and the asterisk (*) denotes the complex conjugate. The active and reactive intensity vectors in a thin plate can now be expressed as follows by taking the real and imaginary parts, respectively:

$$\begin{aligned}\bar{I}(x,y) &= \bar{I}_x(x,y)\,\vec{e}_x + \bar{I}_y(x,y)\,\vec{e}_y \\ \bar{Q}(x,y) &= \overline{Q}_x(x,y)\,\vec{e}_x + \overline{Q}_y(x,y)\,\vec{e}_y\end{aligned} \qquad (5)$$

Motion of a Simply Supported Plate with a Point Load and a Point Damper. Consider a thin elastic plate to which a point damper with a damping coefficient C is attached at the position (x_d, y_d) and a harmonic point force is located at (x_o, y_o) as shown in Fig.1. The plate is simply supported with dimensions $L_x \times L_y$, thickness h, and mass density ρ. For flexural vibration, in-plane forces, rotary inertia and shear deformation effects are not taken into account, since the plate thickness is small relative to the bending wavelength. From the dynamic force and moment equilibria for an elastic thin plate with a point load and a point damper, the governing equation of motion for the transverse displacement $W(x,y,t)$ is expressed as :

$$\tilde{D}\nabla^4 W + \rho h\frac{\partial^2 W}{\partial t^2} + C\frac{\partial W}{\partial t}\delta(x-x_d)\delta(y-y_d) = F_o\delta(x-x_o)\delta(y-y_o)\cos(\omega t-\phi) \qquad (6)$$

where ω is the angular frequency of the applied force. F_o is the amplitude of a simple harmonic point force applied at location (x_o, y_o). $\tilde{D}$, given by $\tilde{D} = D(1+j\eta)$, is the complex dynamic bending rigidity which includes the structural damping, η.

Substituting the displacement $W(x,y,t)$,expressed as Re{ $\tilde{W}(x,y)e^{j\omega t}$ }, into eq. (6) and introducing the wave number k, defined from $\rho h\omega^2/D = k^4$, the damping factor β , defined from $C^2/\rho hD = \beta^4$, and the point force, represented with a complex amplitude $\tilde{F}_o = F_o e^{-j\phi}$, results in :

$$\tilde{D}\nabla^4\tilde{W} - Dk^4\tilde{W} + jD(\beta k)^2\tilde{W}\delta(x-x_d)\delta(y-y_d) = \tilde{F}_o\delta(x-x_o)\delta(y-y_o) \qquad (7)$$

The response for a damped system can be expressed in terms of a series of eigenfunctions of the undamped system. Thus, the complex transverse displacement $\tilde{W}(x,y)$ may be expressed as

$$\tilde{W}(x,y;\omega) = \sum_{m=1}^{\infty}\sum_{n=1}^{\infty}\tilde{B}_{mn}(\omega)W_{mn}(x,y) \qquad (8)$$

where $W_{mn}(x,y) = \sin k_m x \sin k_n y$ is the modal shape function for the m,n mode of a simply supported undamped plate. $k_m = m\pi/L_x$ and $k_n = n\pi/L_y$ are the modal wave numbers, while m and n are the modal indices in the x and y directions, respectively. $\tilde{B}_{mn}(\omega)$ is the complex modal amplitude coefficient to be determined. Substituting the solution in eq. (8) in eq.(7), and using the orthogonality of the eigenfunctions, one obtains:

$$DN(\tilde{k}_{mn}^4 - k^4)\tilde{B}_{mn} + jD(\beta k)^2\left\{W_{mn}^2(x_d,y_d)\tilde{B}_{mn} + \sum_{\substack{p=1\\p\neq m}}^{\infty}\sum_{\substack{q=1\\q\neq n}}^{\infty}W_{mn}(x_d,y_d)W_{pq}(x_d,y_d)\tilde{B}_{pq}\right\} = \tilde{F}_o W_{mn}(x_o,y_o) \qquad (9)$$

where the complex modal wave number $\tilde{k}_{mn}$ is obtained from $\tilde{k}_{mn}^4 = k_{mn}^4(1+j\eta)$, where $k_{mn} = ((m\pi/L_x)^2 + (n\pi/L_y)^2)^{1/2}$.

ACTIVE CONTROL OF STRUCTURAL INTENSITY

To control the power flow (SI) in the plate, a control point force is assumed to act on the plate at the position r_c . Then the SI components in the x- and y-directions can be expressed in terms of the primary and control point forces. With the primary force F_p taken to be real, each component of the active intensity at the error sensor location r_s can be expressed as a quadratic function of the control force, $\tilde{F}_c = F_{cr} + jF_{ci}$, as follows:

$$\bar{I}_x(r_s) = \lambda_{2,x}(F_{cr}^2 + F_{ci}^2) + 2\varphi_{11,x}F_pF_{cr} + 2\varphi_{12,x}F_pF_{ci} + \lambda_{1,x}F_p^2$$
$$\bar{I}_y(r_s) = \lambda_{2,y}(F_{cr}^2 + F_{ci}^2) + 2\varphi_{11,y}F_pF_{cr} + 2\varphi_{12,y}F_pF_{ci} + \lambda_{1,y}F_p^2 \quad (10)$$

After some rearrangement, the intensity component can be rewritten as :

$$\bar{I}_x(r_s) = \lambda_{2,x}\{(F_{cr} - F_{cr,x})^2 + (F_{ci} - F_{ci,x})^2 - S_x^2\}$$
$$\bar{I}_y(r_s) = \lambda_{2,y}\{(F_{cr} - F_{cr,y})^2 + (F_{ci} - F_{ci,y})^2 - S_y^2\} \quad (11)$$

where $F_{cr,x} = -\dfrac{\varphi_{11,x}}{\lambda_{2,x}}F_p \qquad F_{ci,x} = -\dfrac{\varphi_{12,x}}{\lambda_{2,x}}F_p$

$$F_{cr,y} = -\frac{\varphi_{11,y}}{\lambda_{2,y}}F_p \qquad F_{ci,y} = -\frac{\varphi_{12,y}}{\lambda_{2,y}}F_p$$

$$S_x^2 = -\frac{\lambda_{1,x}\lambda_{2,x} - (\varphi_{11,x}^2 + \varphi_{12,x}^2)}{\lambda_{2,x}^2}F_p^2$$

$$S_y^2 = -\frac{\lambda_{1,y}\lambda_{2,y} - (\varphi_{11,y}^2 + \varphi_{12,y}^2)}{\lambda_{2,y}^2}F_p^2$$

The terms $\lambda_{1,x}$, $\lambda_{1,y}$ are functions of the positions of the primary force and the error sensor that contribute to the x- and y- components of I, respectively, and $\lambda_{2,x}$, $\lambda_{2,y}$ are those for the control force and the error sensor. The terms $\varphi_{11,x}$, $\varphi_{12,x}$,and $\varphi_{11,y}$, $\varphi_{12,y}$ are functions of the positions of the primary force, the control force, and the error sensor, which appear in the x- and y- components of I.

Minimization of the Structural Intensity. The magnitude of the active intensity vector to be minimized is $J = |I| = \sqrt{\bar{I}_x^2 + \bar{I}_y^2}$, where each of the two components of I is quadratic in the control force . Then |I| is of fourth power in terms of the control force. Thus, differentiation of |I| with respect to the control force would lead to nonlinear equations of the third degree in the control force. This is in marked contrast to control of SI, or the vibration levels in beams. Differentiating the magnitude of the structural intensity in terms of the real and imaginary components of the control force, and setting both derivatives to zero yields the optimal control force. Thus, the optimal control force is calculated by solving two nonlinear simultaneous equations of third degree in the real and the imaginary components of the control force:

$$\frac{\partial J}{\partial F_{cr}} = \alpha_1 F_{cr}^3 + \alpha_2 F_{cr}^2 + \alpha_3(F_{ci})F_{cr} + \alpha_4(F_{ci}) = 0$$
$$\frac{\partial J}{\partial F_{ci}} = \beta_1 F_{ci}^3 + \beta_2 F_{ci}^2 + \beta_3(F_{cr})F_{ci} + \beta_4(F_{cr}) = 0 \quad (12)$$

where the α's and β 's are functions of the terms in eq.(11). If the following conditions are satisfied,

$$\varphi_{11,x}^2 + \varphi_{12,x}^2 \geq \lambda_{1,x}\lambda_{2,x}$$
$$\varphi_{11,y}^2 + \varphi_{12,y}^2 \geq \lambda_{1,y}\lambda_{2,y} \tag{13}$$

then there exists a set of optimal control forces which make the magnitude of each of the two components of the active intensity at the error sensor position zero individually. Their trajectories are expressed as equations of circles as follows:

$$(F_{cr} - F_{cr,x})^2 + (F_{ci} - F_{ci,x})^2 = S_x^2$$
$$(F_{cr} - F_{cr,y})^2 + (F_{ci} - F_{ci,y})^2 = S_y^2 \tag{14}$$

If the two optimum control force solutions, forming two circles that nullify the Ix and Iy intensities, intersect, then there exist two intersection points for these two circles. This occurs if the following condition is satisfied :

$$\left|S_x - S_y\right| \leq \sqrt{(F_{cr,x} - F_{cr,y})^2 + (F_{ci,x} - F_{ci,y})^2} \leq S_x + S_y \tag{15}$$

In this case, there exist two possible solutions for the optimal control force that make each component of intensity zero simultaneously such that the intensity magnitude will be zero. They are obtained by solving eq.(14) as follows:

$$F_{oi} = \frac{\{(F_{ci,y}K_1 + F_{ci,x}K_2) - (F_{ci,y} - F_{ci,x})K_3\} \pm \sqrt{(F_{ci,y}K_1 + F_{ci,x}K_2)^2 - (F_{cr,y} - F_{cr,x})^2 K_4}}{K_1 + K_2}$$
$$F_{or} = -\frac{(F_{ci,y} - F_{ci,x})F_{oi} + K_3}{F_{cr,y} - F_{cr,x}} \tag{16}$$

where
$$K_1 = F_{cr,x}^2 + F_{ci,x}^2 - (F_{cr,x}F_{cr,y} + F_{ci,x}F_{ci,y})$$
$$K_2 = F_{cr,y}^2 + F_{ci,y}^2 - (F_{cr,x}F_{cr,y} + F_{ci,x}F_{ci,y})$$
$$K_1 + K_2 = (F_{cr,y} - F_{cr,x})^2 + (F_{ci,y} - F_{ci,x})^2$$
$$K_3 = \frac{1}{2}\{\frac{\lambda_{1,x}}{\lambda_{2,x}} - \frac{\lambda_{1,y}}{\lambda_{2,y}}\}F_p^2 \tag{17}$$
$$K_4 = \frac{\lambda_{1,x}}{\lambda_{2,x}}F_p^2K_2 + \frac{\lambda_{1,y}}{\lambda_{2,y}}F_p^2K_1 + K_3^2$$

The degree of coupling between the primary and control forces is different for the x- and the y-components of the active intensity. When the following conditions are satisfied,

$$\varphi_{11,x}^2 \geq \lambda_{1,x}\lambda_{2,x}$$
$$\varphi_{11,y}^2 \geq \lambda_{1,y}\lambda_{2,y} \tag{18}$$
$$\left(\frac{\lambda_{2,x}}{\lambda_{1,x}} - \frac{\lambda_{2,y}}{\lambda_{1,y}}\right)^2 = \left(\frac{2\varphi_{11,x}}{\lambda_{1,x}} - \frac{2\varphi_{11,y}}{\lambda_{1,y}}\right)\left(\frac{2\varphi_{11,y}}{\lambda_{1,y}}\frac{\lambda_{2,x}}{\lambda_{1,x}} - \frac{2\varphi_{11,x}}{\lambda_{1,x}}\frac{\lambda_{2,y}}{\lambda_{1,y}}\right)$$

then one of the numerators of eq. (18) becomes zero. Thus, one of the two possible optimal control force solutions has only a real part, and the other one has a complex value as follows :

$$F_{oi,1} = 0$$

$$F_{or,1} = -\frac{\dfrac{\lambda_{1,x}}{\lambda_{2,x}} - \dfrac{\lambda_{1,y}}{\lambda_{2,y}}}{\dfrac{2\varphi_{11x}}{\lambda_{2,x}} - \dfrac{2\varphi_{11y}}{\lambda_{2,y}}} F_p \qquad (19a)$$

$$F_{oi,2} = \frac{\{(F_{ci,y}K_1 + F_{ci,x}K_2) - (F_{ci,y} - F_{ci,x})K_3\}}{K_1 + K_2}$$

$$F_{or,2} = -\frac{(F_{ci,y} - F_{ci,x})F_{oi,2} + K_3}{F_{cr,x} - F_{cr,x}} \qquad (19b)$$

NUMERICAL RESULTS

Consider a steel plate that has the dimensions 0.60x0.40x0.0032 m., density 7800 Kg/m3, and Young's modulus of 2.06x10E11 N/sq. m. A 1N point force is located at (0.15, 0.15m), and a point damper located at (0.50, 0.10m).

To investigate the influence of the structural damping on the SI of an internally damped plate, the SI is computed before control for resonance and off resonance frequencies. At resonance, the power flows from the source to the regions of maximum velocity in the uncontrolled plate because the internal energy absorption depends on the damping coefficient and the local kinetic energy. This can be seen clearly by examining the displacement field of Fig.2(a) and comparing it to the SI vector map in Fig.3 for the uncontrolled plate without a point damper at the resonance frequency of the (2,2) mode,(280 Hz). In fact, the total injected power from the primary source without control, 9.54×10^{-3} Nm/sec, is exclusively absorbed by the plate's internal damping as shown in Table 1.

To investigate the power flow in an internally damped plate without a point damper controlled at resonance, the optimal control force, calculated for an error sensor located near the damper position, was found to be F=-0.783-j0.021 N. With this control force, the SI vector map is shown in Fig. 4. It can be seen that after control, the displacement field has been changed so that the nodal lines of the (2,2) uncontrolled mode have shifted and the regions of the maximum velocities or the kinetic energy has shifted as shown in Fig.2(b). Thus, one can see that power flows from the point source to the regions of maximum kinetic energy. However, the total input power by the primary and control forces has dropped significantly from the uncontrolled 9.54×10^{-3} Nm/sec to the controlled 1.48×10^{-5} Nm/sec. Thus, the total injected power is absorbed by the plate exclusively and hence it also has dropped to 1.48×10^{-5} Nm/sec (See Table 1).

One can thus conclude that for a plate without an absorbent point attachment (point damper), the control algorithm to minimize the SI at an error sensor in essence changes the displacement field in order to maximize the kinetic energy at other locations, thereby diverting the SI flow to those locations away from the error sensor.

To investigate the combined role of the internal damping and the point damper before and after control, the SI maps were computed for C=200 Nm/sec and η=0.01. The SI map before control at the resonance frequency of 280 Hz, the (2,2) mode, is shown in Fig.5 and shows that the power flows to both the point damper and the regions of maximum kinetic energy (See Fig.2(a)), as explained before. For this case, the total injected power from the primary source,(1.48×10^{-3} Nm/sec), is split between the plate internal absorption (0.27×10^{-3} Nm/sec) and the point damper (1.21×10^{-3} Nm/sec) (See Table 1). After control, with the optimal control force

F=-0.782-j0.012N, the total injected power by the primary and control forces has significantly dropped from the uncontrolled case, i.e. from 1.48×10^{-3} Nm/sec to 1.07×10^{-3} Nm/sec, see Table 1. The SI map for the controlled case is shown in Fig. 6. It can be seen that the power , while very small, flows from the primary and control forces to the regions of maximum kinetic energy (1.07×10^{-5} Nm/sec) and to the point damper (4.17×10^{-9} Nm/sec). In essence, the control algorithm which required the minimization of the SI near the damper has been very effective in that the control of SI near the damper diverted most of the injected power to the areas of the maximum internal damping.

Thus, one can conclude that if the control algorithm requires the minimization of the energy flow to a point damper, the injected power is exclusively absorbed by the plate only, as if the point damper does not exist. This is accomplished by changing the displacement field in order to maximize the kinetic energy at other regions away from the point damper.

To investigate the influence of resonance vs. off-resonance excitation on the control of SI, the SI maps were computed for the frequency of 280 Hz, which is the resonance frequency of the uncontrolled (2,2) mode and for the off resonance frequency at 180 Hz, which falls between the (1,2) and (2,1) modes. With an internal damping loss factor η=0.01 and a point damper C=200 Nsec/m, the SI map for off-resonance at 180 Hz is shown in Fig. 7. First, the overall response of the plate at the off resonance frequency of 180 Hz is very small and hence the total injected power which is absorbed by the plate and the point damper is expected to be low (1.34×10^{-4} Nm/sec) when compared to the resonance excitation at 280 Hz, with the injected power of 1.48×10^{-3} Nm/sec (see Table 2). However, the injected power is again split between the plate internal damping and the point damper in either case.

For optimal control at the off resonance frequency of 180 Hz, the SI map is shown in Fig.8. For off resonance excitation, an optimal control force of F=-1.212-j0.007 N results in a total injected power of (0.8×10^{-5} Nm/sec), which is about the same as the resonance case. However, since the error sensor was located near the point damper, most of the energy was diverted again to the regions with maximum kinetic energy, see Fig.9(b).

CONCLUSIONS

The parametric study on the control of SI at the point damper led to a number of conclusions:

*It was found that control of the components Ix or Iy is not sufficient to control the total SI at the damper. The control of $|\mathbf{I}|$ was essential to nullify or minimize the power flow to the damper.

*Control of the SI at the damper through an actuator located near the primary source altered the modal characteristics of the uncontrolled mode to achieve the required minimization.

*Control of the power flow in an internally damped plate without a point damper showed that the energy flows from the primary source to areas of maximum kinetic energy, where internal absorption is maximum.

*When the primary source excitation is at a resonance frequency and the actuator is in the nearfield of the source, the SI is minimized over the entire plate, i.e. it has a global control property.

*When the primary source excitation is at an off-resonance frequency, the displacement field is altered by the control source in order to divert the energy to regions of maximum kinetic energy.

*Control algorithm based on minimizing SI was more effective than that for displacement control.

*At resonance, the SI or displacement reduction due to the control source increases with decreasing internal damping coefficient η or point damper coefficient C.

*The total input power reduction, which is a measure of the efficiency of the control mechanism, increases with decreasing C or η.

REFERENCES

1. Noiseux, D. U., "Measurement of Power Flow in Uniform Beams and Plates," J. Acoust. Soc. Am., 47(2), pp 238-247, (1970).
2. Pavic, G.,"Measurement of Structure Born Wave Intensity Part I: Formulation of the Methods," Journal of Sound and Vibration, 49, 221-230,1976.
3. Cuschieri,J. M., "Experimental Measurement of Structural Intensity on an Aircraft Fuselage," J. Noise Control Eng., 37(3) ,97-107,1991.
4. Verheij, J. W., "Cross Spectral Density Methods for Measuring Structure Borne Power Flow on Beam s and Pipes," Journal of Sound and Vibration, 70(1),133-139,(1980).
5. Hayek, S. I., M. J. Pechersky and B. C. Suen, " Measurement and Analysis of Near and Far Field Structural Intensity by Scanning Laser Vibrometry," Proc. International Congress on Intensity Techniques, Senlis, France, 27-29 April, 1990.
6. Williams, E.G., H. D. Dardy, R. G.Fink, " A Technique for Measurement of Structure-Borne Intensity in Plates," J. Acoust. Soc. Am., 78(6), 2061-2068, (1985).
7. Pan, J. and C. H. Hansen, "Active Control of Total Vibratory Power Flow in a Beam. I : Physical System Analysis," J. Acoust. Soc. Am. 89(1), 200-208, January 1991.
8. Swanson, D.C., C. Gentry, S. I. Hayek, and S.D. Sommerfeldt, " Adaptive control of bending waves in a finite beam", J. Acoust. Soc. Amer. 94(3), 1817A, 1993
9. Gentry, C., "Investigation of Adaptive Intensity Control Methods for a Finite Beam," M.S. Thesis, The Pennsylvania State University, University Park, PA, 16802, June. 1993.
10. Pavic, G., "Power Suppression of Vibrating Infinite Beams and Plates by Secondary Sources," Proc. of the Inst. of Acoustics, 15(3), 395-402,1993.
11. Pan, J. and Hansen, C., "Active Control of Total Power Flow along a Beam" ,Proc. International Congress on Recent Development in Air-and Structure-borne Sound and Vibration," Auburn University, Alabama, 229-236, 1990.
12. Brennan, M. J., Elliott, S.J., and Pinnington, R.J., "Power Absorption and Minimization on Euler-Bernoulli Beams," Proc. Internoise 93, Leuven, Belgium, Aug. 24-26,1993, 851-854.
13. Miller, D. W., S.R. Hall and A.H. von Flotow, "Optimal Control of Power Flow at Structural Junctions," J. Sound and Vibration, 140,475-497,1990.
14. Gonidou, L.O., "Active Control of Flexural Power Flow in a Beam," MS.. Thesis, VPI and S U, Blacksburg, VA, 1988.
15. Rae, D., " Active Feedforward Vibration Control of Beams with Impedance Terminations", MS.. thesis, Penn State University, University Park, PA ,16802, 1995.
16. Tanaka, N., S. D. Snyder, Y. Kikushima, and M. Kuroda, "Vortex Structural Power Flow in a Thin Plate and the Influence on the Acoustic Field," J. Acoust. Soc. Am., 96(3),2563-1574, 1994.
17. Redman-White, W., P.A. Nelson, A.R.D. Curtis, "Experiments on the Active Control of Flexural Wave Power Flow," Journal of Sound and Vibration ,112(1),187-191, 1987.
18. Fuller, C. R., and G. Gibbs, "Simultaneous Active Control of Flexural and Extensional Waves in Beams," J. of Intelligent. Mater. Systems. and Structures., 1, 235-247, 1990.
19. Schwenk, A. E., S. D. Sommerfeldt, and S. I. Hayek, "Adaptive Control of Structural Intensity Associated with Bending Waves in a Beam," J. Acoust. Soc. Am. 96(5) 2826-2835, 1994.
20. Fuller, C. R., Gibbs, G. P., and Gonidou, L.O., "Application of Power and Impedance Measurement Techniques to the Study of Active Control of Flexural Energy Flow in Beams," Proc. International Congress on Intensity Techniques, Senlis, France, 27-29 April, 1990.

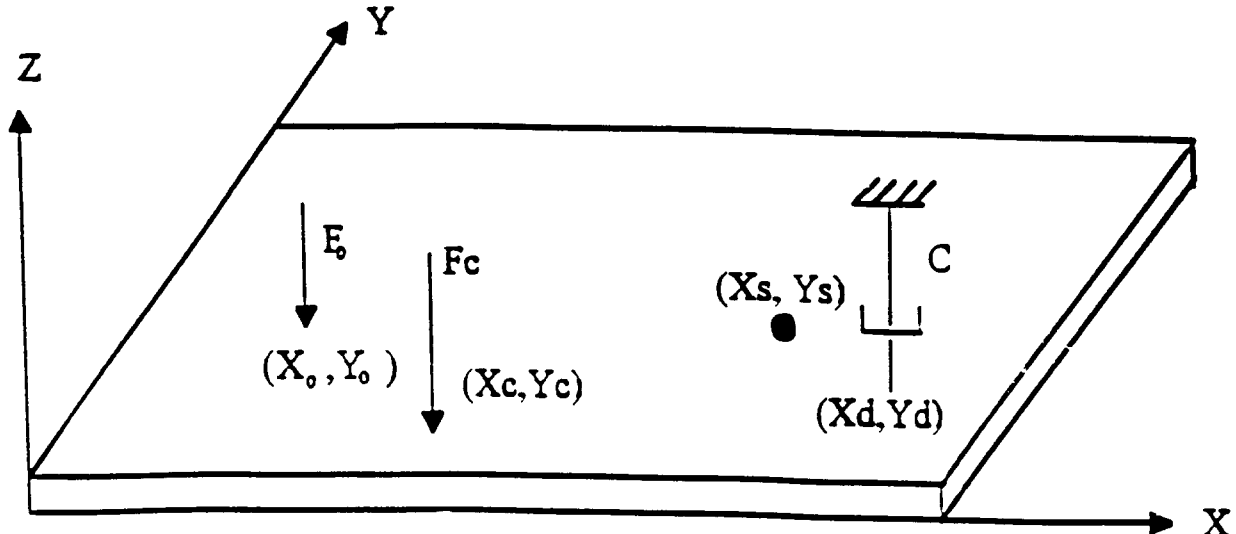

Fig. 1 Simply Supported Plate with Point Force,Control Force,Error Sensor,and Point Damper

Table 1. Dynamic Response depending on the Damping Loss Factor η of the Simply Supported Plate and the Damping Coefficient C of an attached Point Damper for control at 280 Hz.

damping factor / variables	C=200Nm/sec η=0		C=0 Nm/sec η=0.01		C=200Nm/sec η=0.01	
	before control	after control	before control	after control	before control	after control
control force(N)	-	-0.783	-	- 0.7832-j0.002		- 0.782-j0.012
intensity at damper(N/sec)	5.87×10^{-3}	0	1.25×10^{-2}	1.96×10^{6}	4.43×10^{-3}	2.60×10^{-6}
displacement at damper(m)	2.33×10^{-6}	0	1.33×10^{-5}	1.32×10^{-7}	1.97×10^{-6}	3.67×10^{-9}
injected power at primary source(Nm/sec)	1.67×10^{-3}	3.36×10^{-16}	9.54×10^{-3}	6.23×10^{-6}	1.48×10^{-3}	9.51×10^{-6}
injected power at secondary source(Nm/sec)	-	-3.36×10^{-16}	-	8.55×10^{-6}		1.16×10^{-6}
total input power(Nm/sec)	1.67×10^{-3}	0	9.54×10^{-3}	1.48×10^{-5}	1.48×10^{-3}	1.07×10^{-5}
absorbed power at damper(Nm/sec)	1.67×10^{-3}	0	-	-	1.21×10^{-3}	4.17×10^{-9}
energy flow rate through the plate (Nm/sec)	0	0	9.54×10^{-3}	1.48×10^{-5}	0.27×10^{-3}	1.07×10^{-5}

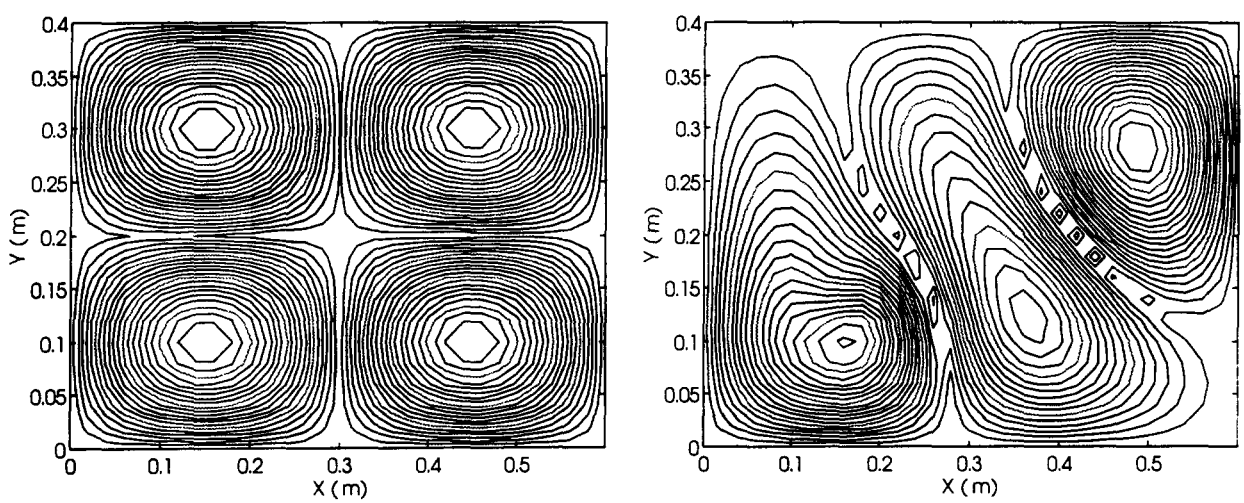

(a) (b)

Fig. 2 Displacement Contour (a) before Control (Max. 1.53×10^{-5} m, at Damper 1.33×10^{-5} m) (b) after Control(Max. 7.23×10^{-7} m, at Damper 1.32×10^{-7} m), Control Force Fc=-0.7832-j0.002N, 280Hz, C=0, η=0.01

Table 2. Dynamic Response Depending on the Excitation Frequency for Control in the simply supported plate (η =0.01) with an Attached Point Damper (C=200 Nm/sec)

frequency / variables	280 Hz resonant frequency		180 Hz non-resonant frequency	
	before control	after control	before control	after control
control force(N)	-0.782-j0.012		- 1.212 -j0.007	
intensity at damper(N/sec)	4.43×10^{-3}	2.60×10^{-6}	4.32×10^{-4}	9.64×10^{-8}
displacement at damper(m)	1.97×10^{-6}	3.67×10^{-9}	9.41×10^{-7}	8.01×10^{-9}
injected power at primary source(Nm/sec)	1.48×10^{-3}	9.51×10^{-6}	1.34×10^{-4}	-5.21×10^{-6}
injected power at secondary source(Nm/sec)	-	1.16×10^{-6}	-	1.32×10^{-5}
total input power(Nm/sec)	1.48×10^{-3}	1.07×10^{-5}	1.34×10^{-4}	0.8×10^{-5}
absorbed power at damper(Nm/sec)	1.21×10^{-3}	4.17×10^{-9}	1.13×10^{-4}	8.21×10^{-9}
energy flow rate through the plate (Nm/sec)	0.27×10^{-3}	1.07×10^{-5}	0.21×10^{-4}	8.02×10^{-6}

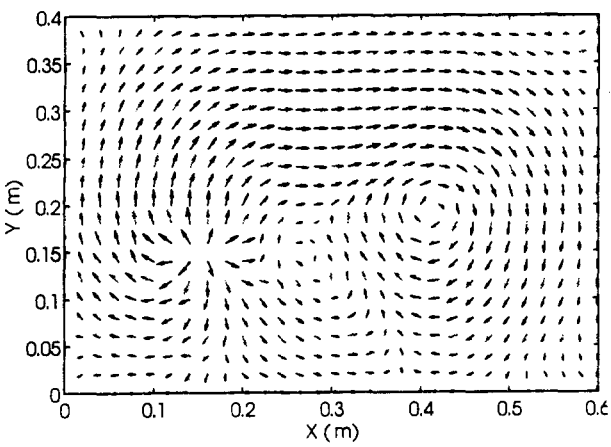

Fig. 3 Normalized SI Vector Map. before Control (Max. 7.82×10^{-2} N/sec), 280Hz, C=0, η=0.01

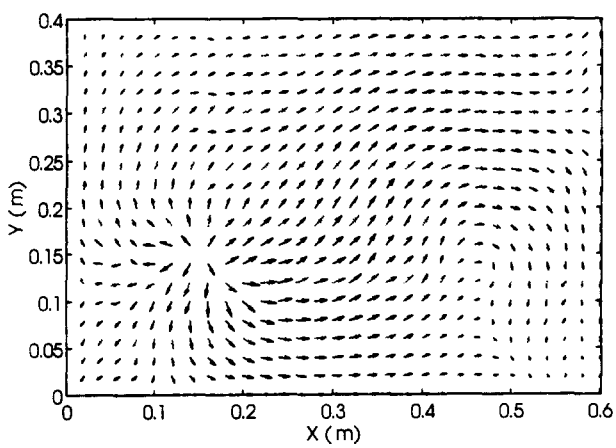

Fig. 4 Normalized SI Vector Map. after Control(Max. 1.11×10^{-4} N/sec), Fc=-0.7832-i0.002N,280Hz, C=0, η=0.01

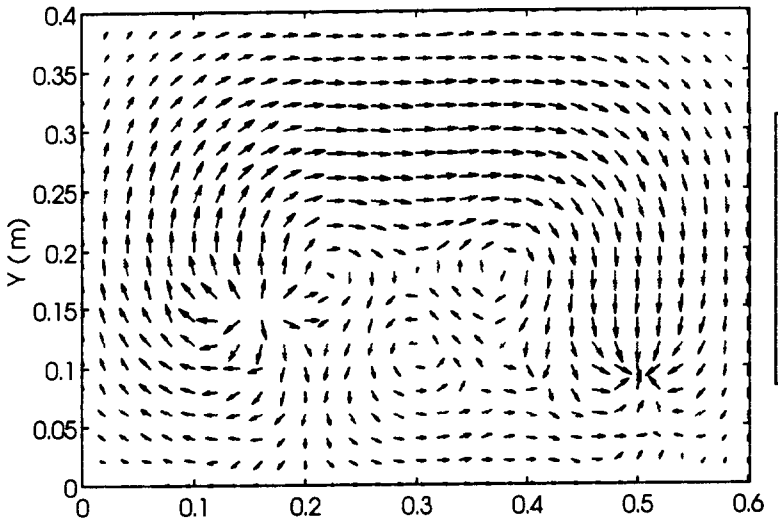

Fig. 5 Normalized SI Vector Map. before Control, (Max. 1.43×10^{-2} N/sec), 280 Hz,C=200Nsec/m, η=0.01

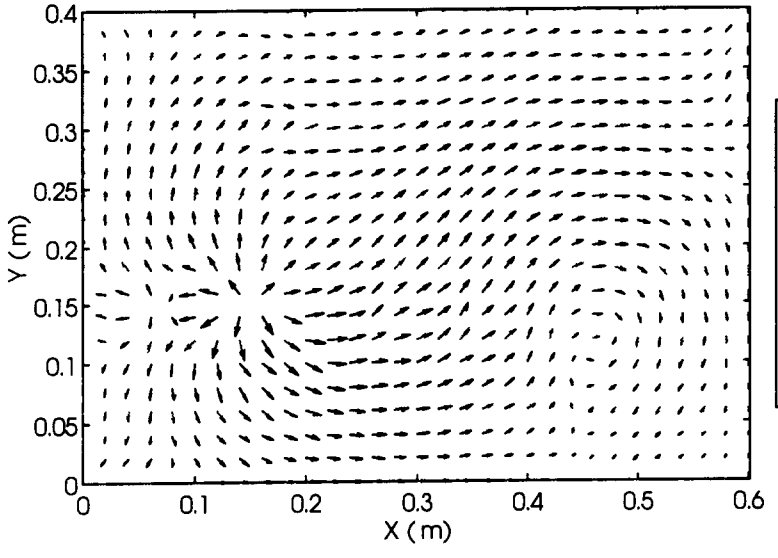

Fig. 6 Normalized SI Vector Map. after Control, (Max. 1.43×10^{-2} N/sec), 280 Hz,C=200Nsec/m, η=0.01, Fc=-0.8722-j0.012N

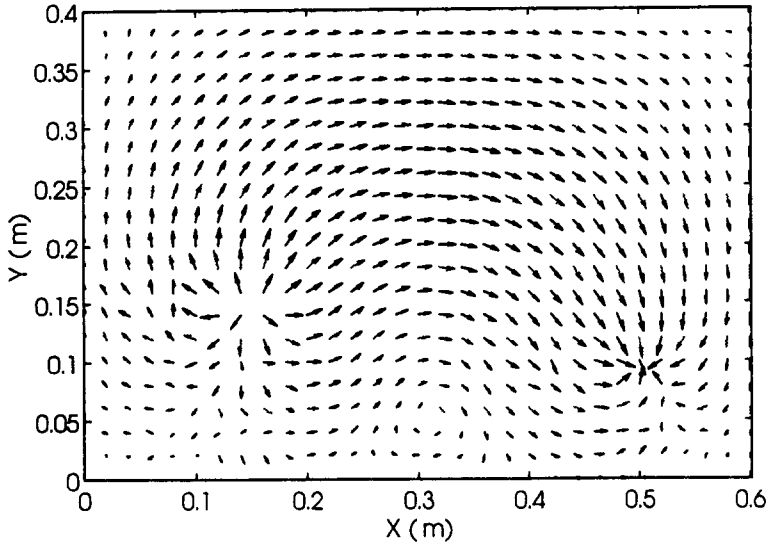

Fig. 7 Normalized SI Vector Map. before Control, (Max. 1.36×10^{-3} N/sec), 180 Hz,C=200Nsec/m, η=0.01

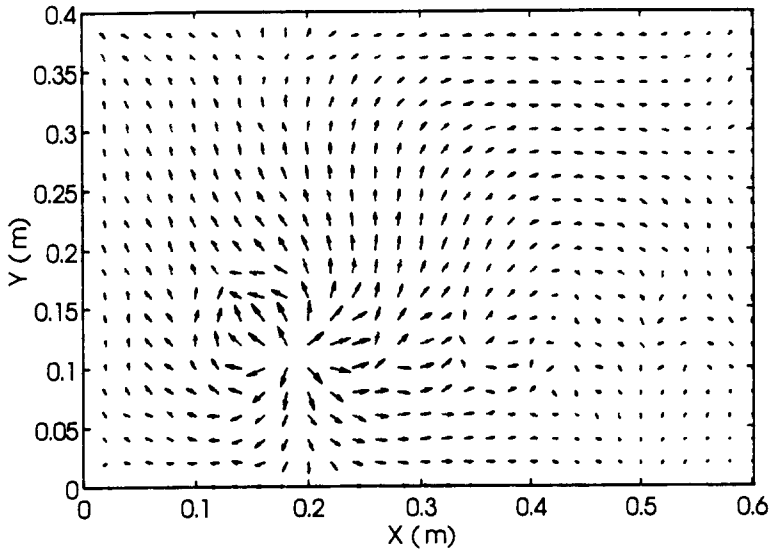

Fig. 8 Normalized SI Vector Map after Control. 180Hz, η=0.01, C=200Nsec/m, Fc=-1.294-j0.008N, Max. 1.44×10^{-4} N/sec

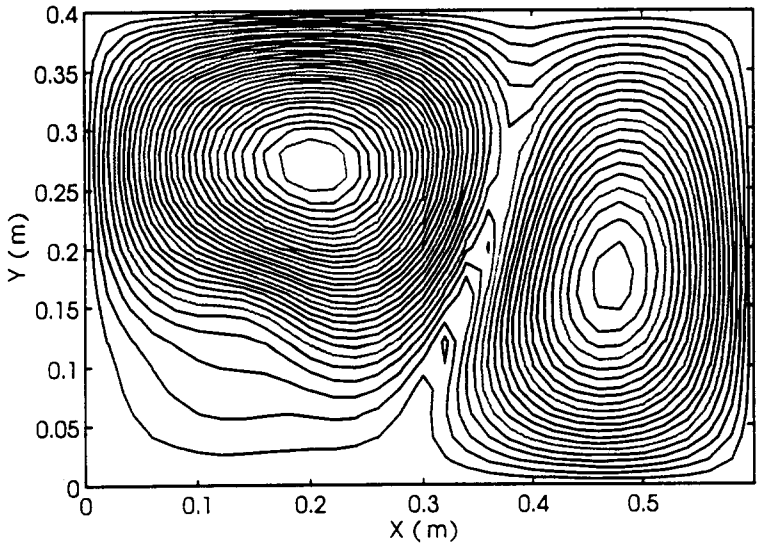

Fig. 9(a) Displacement Contour. before Control, (Max. 1.79×10^{-6}m, at Damper 9.41×10^{-7} m), 180Hz, η=0.01, C=200Nsec/m

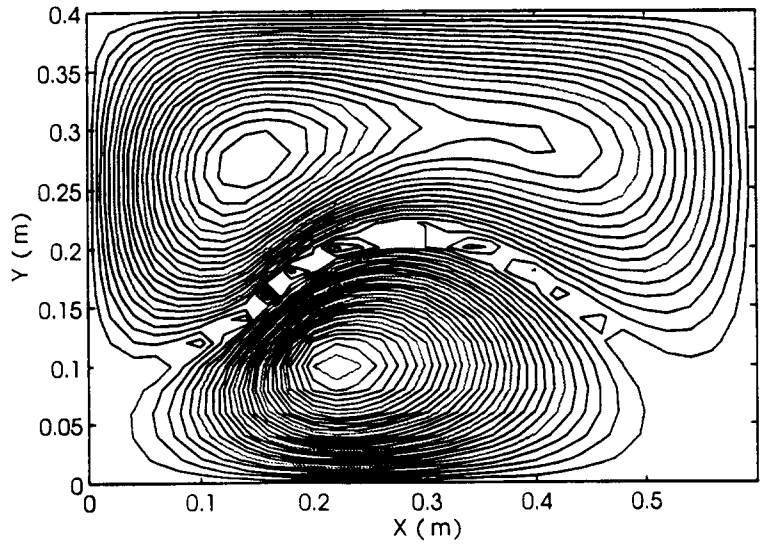

Fig. 9(b) Displacement Contour. After Control, (Max. 1.04×10^{-6}m, at Damper 2.33×10^{-9} m), Fc=-1.294-j0.008N, 180Hz, η=0.01, C=200Nsec/m